Berkala **PENELITIAN HAYATI**

ISSN: 08526834 | E-ISSN:2337-389X

Volume 32 | No. 2 | **August** | 2026

Original article

In Silico Evaluation of *Leucaena leucocephala* Seed Phytochemicals as Potential inhA Inhibitors Against Tuberculosis

Zelika Melnawati[1], Putri Rosfiana Dewi[1], Isda Nur Fitriyah[1], Fiko Dalili Sharfina[1] and Junairiah[1*]

[1] Department of Biology, Faculty of Science and Technology, Universitas Airlangga. Jl. Mulyorejo, Surabaya 60115, East Java, Indonesia

Abstract

Tuberculosis (TB), caused by *Mycobacterium tuberculosis* (Mtb), remains one of the world's most concerning infectious diseases due to rising incidence. The enoyl-acyl carrier protein reductase (InhA), a key enzyme in the fatty acid synthase II pathway, is a validated target for anti-TB drug discovery as it catalyzes mycolic acid biosynthesis in the Mtb cell wall. This study aimed to evaluate the inhibitory potential of bioactive compounds derived from *Leucaena leucocephala* seeds against the InhA protein using *in silico* molecular docking. A total of 73 phytochemicals were screened for drug-likeness and toxicity profiles, resulting in the selection of 11 compounds for docking analysis. Diethyl phthalate (DEP) emerged as the most favorable hit against InhA (binding affinity −7.5 kcal·mol^{-1}), forming a conventional hydrogen bond with GLY96 and multiple stabilizing hydrophobic contacts (PHE41, ILE95, VAL65). PASS predictions supported moderate antimycobacterial probability for several hits (e.g., DEP Pa ≈ 0.33). MD analysis yielded an average RMSF of 0.819 Å for the DEP–InhA complex, with localized residue fluctuations (>3 Å) in flexible loop and N-terminal regions, indicating borderline dynamic stability of the bound pose.The study suggests that phytochemicals from *L. leucocephala* seeds may offer safe, natural compounds with potential relevance to anti-tuberculosis research and could serve as a basis for further *in vitro* and *in vivo* exploration.

Keywords: *Leucaena leucocephala***,** diethyl phthalate, InhA, *In silico*, anti-tuberculosis

Received: October 27, 2025 | Revised: August 28, 2026 | Accepted: August 30, 2026

Introduction

Mycobacterium tuberculosis (Mtb) is the causative agent of the infectious disease tuberculosis (TB). Tuberculosis is considered one of the most concerning diseases recorded by the World Health Organization (WHO), with a total of 10,6 million cases worldwide in 2021 (WHO, 2022). An estimated one-quarter of the global population is infected with Mtb, and 5–10% of infected individuals are also capable of transmitting the disease (WHO, 2020). The WHO further reported that developing countries, including Indonesia, are among the largest contributors to the increase in TB cases in 2020 and 2021 (WHO, 2023). The prevalence of TB rose by approximately 0.4 million cases, primarily affecting individuals aged 45 to 54 years, with 969,000 cases and 93,000 TB-related deaths recorded annually, equivalent to 11 patient deaths every hour (WHO, 2022).

One of the most promising molecular targets against Mtb is Enoyl Acyl Carrier Protein Reductase (InhA), a key enzyme in the FAS-II pathway that plays a crucial role in fatty acid biosynthesis, particularly in the production of mycolic acids essential components of the Mtb cell wall (Xia *et al*., 2018). The FAS-II pathway has long been recognized as a valuable target for drug discovery, providing opportunities for selective action with novel antibacterial agents (Pajk *et al*., 2016). InhA, a NADH-dependent enzyme, is currently inhibited by the first-line antimycobacterial drug isoniazid; however, the growing resistance to isoniazid highlights the urgent need to identify new compounds that can effectively inhibit this enzyme (Sink *et al*., 2015).

The lamtoro tree or Leucaena (*Leucaena leucocephala*) is a coniferous tree species belonging to the family Fabaceae and subfamily Mimosoideae, which comprises 32 species (Bageel *et al*., 2020). The seeds of *L. leucocephala* contain lipids, arginine, alanine, cysteine, glutamic acid, isoleucine, leucine, lysine, methionine, and carbohydrates (Verma *et al*., 2018). The anti-tuberculosis potential of this plant and its bioactive compounds represents one of the approaches to developing potential drugs to suppress tuberculosis in endemic countries, including Indonesia, which has high biodiversity. Research and evaluation of active compounds are designed to address antibacterial tuberculosis. Natural bioactive compounds are explored as candidates to inhibit and reduce infections caused by Mtb through *in silico* molecular docking.

The aim of this study was to evaluate the inhibitory potential of *L. leucocephala* bioactive compounds against target proteins in Mtb through binding affinity analysis using an *in silico* assay. This research is expected to contribute to the discovery of anti-tuberculosis drugs and provide insights for the community to utilize natural products in daily consumption as a preventive measure against tuberculosis.

* Corresponding Author:

Junairiah
Department of Biology, Faculty of Science and Technology, Universitas Airlangga. Jl. Mulyorejo, Surabaya 60115, East Java, Indonesia
E-mail: junairiah@fst.unair.ac.id

http://dx.doi.org/10.23869/bphjbr.32.2.20262

Published by © PBI East Java. Open Access www.berkalahayati.org

Methods

This research is computationally based, utilizing online data and software to support molecular docking analysis. Bioactive compounds from *L. leucocephala* seeds were obtained based on a study of scientific journal literature and served as ligands in this study. Compound ID (CID) and Simplified Molecular-Input Line-Entry System (SMILE) data collection were obtained from the PubChem website (https://pubchem.ncbi.nlm.nih.gov/). The target protein used as a receptor, inhA from Mtb (PDB ID: 2ie0), was taken from the RCSB Protein Data Bank (https://www.rcsb.org/) (Fig.1). In this study, the protein structure used for molecular docking was the wild-type InhA (PDB ID: 2IE0), which represents the native, drug-sensitive form of the enzyme. This selection aligns with the objective of identifying potential inhibitor candidates that can interact optimally with the normal catalytic site of InhA. No mutant InhA structures were included in this study, as the present work focuses on an initial in silico screening of ligand binding to the native enzyme.

The structure of the drug compound isoniazid (HMDB0015086) as a control was collected from the Human Metabolome Database (HMDB) website (https://www.hmdb.ca/) (Fig. 2). Drug similarity was evaluated using SwissADME (http://www.swissadme.ch). The toxicity profiles of selected compounds were predicted using ProTox 3.0. Molecular docking and visualization were performed using PyRx 0.8 and BIOVIA Discovery Studio Visualizer 2020, respectively.

This research employed a descriptive observational design to evaluate the binding affinity of bioactive compounds from *L. leucocepha* seeds against the inhA protein through a one-shot pre-experimental *in silico* approach.

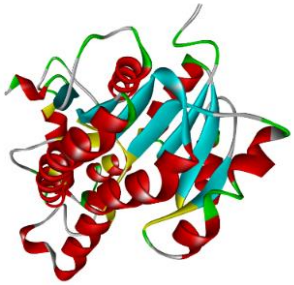


Fig. 1 The inhA protein of *M. tuberculosis* that has been cleaned

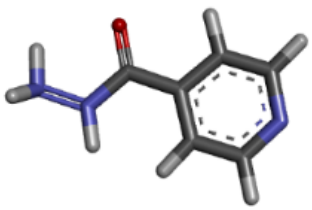


Fig. 2 Control ligan isoniazid (HMDB0015086)

Retrieval and Optimization of *L. leucocephala*-Derived Ligand

Data collection of bioactive compounds from L. leucocephala seeds was obtained from several scientific journal publications published over the past five years, namely Elbanoby *et al*. (2022); Chargui *et al*. (2023); Verma *et al*. (2018); Nadhm dan Al-Waheeb, (2024), where all journals showed the ability in antibacterial. These compounds were then subjected to CID data collection and SMILE information retrieval from the PubChem website for further use in subsequent stages (Kautsar *et al.*, 2024). The structure of the control ligand, the drug compound isoniazid, was also collected from the HMDB website in .pdb format.

Retrieval and Optimization of inhA Protein Structure

The inhA protein structure was obtained from the RCSB PDB Database website and downloaded in .pdb format. The receptor structure was sterilized using BIOVIA Discovery Studio Visualizer software to remove cofactors, solvents, and binding ligands from the protein structure. The sterilized structure was saved as a .pdb file and a 3D image (Kautsar *et al.*, 2024). The wild-type InhA structure was intentionally selected, and mutant InhA variants associated with isoniazid resistance were not included, as this study aimed to provide a baseline evaluation of ligand binding at the native catalytic site. The InhA crystal structure (PDB ID: 2IE0) contains a co-crystallized NADH molecule, which functions as the natural cofactor of the enzyme. During protein preparation, NADH and all non-protein molecules were removed to obtain a clean receptor structure and allow unbiased docking of the test ligands and the reference compound.

Drug-Likeness Evaluation

Assessment of the drug-like characteristics of plant-derived compounds is a crucial step in the drug discovery process. Lipinski's Rule of Five is a widely used guideline for predicting the absorption and distribution of compounds in the human body. The main criteria include a molecular weight (MW) ≤500 Da, log P ≤5, a hydrogen bond donor (HD) ≤5, and a hydrogen bond acceptor (HA) ≤10. Assessment of Absorption, Distribution, Metabolism, and Excretion (ADME) showed that most compounds met Lipinski's criteria. Candidate drug-like compounds must have a virulence score of 0 or 1. Testing was conducted on the SwissADME website (Yuliana *et al.*, 2025).

Toxicity Evaluation

Toxicity evaluation using an *in silico* approach to assess the safety of selected compounds. This method is used to examine and identify toxicity profiles, capturing information on acute toxicity classes (predicted median lethal dose (LD50) in mg/kg body weight and toxicity classes. Toxicity class categories include: Class I (LD50 ≤ 5, fatal if swallowed); Class II (5 < LD50 ≤ 50, also fatal if swallowed); Class III (50 < LD50 ≤ 300, toxic if swallowed); Class IV (300 < LD50 ≤ 2000, harmful if swallowed); Class V (2000 < LD50 ≤ 5000, potentially harmful if swallowed); and Class VI (LD50 > 5000, considered non-toxic). Compounds included in class VI will be selected as test ligands for docking. Toxicity analysis was performed using the ProTox 3.0 website (Raies dan Bajic, 2016; Banerjee *et al.*, 2024).

Antimycobacterial and Antituberculosis Probability Prediction

The biological activities were predicted using the PASS Online web server (http://way2drug.com/PASSOnline/). The predictions focused specifically on Antimycobacterial and Antituberculosis activities. PASS results are expressed as Pa (probability "to be active"), which estimate the likelihood that each compound exhibits or lacks a given biological activity. Compounds with Pa > 0.3 were considered to have meaningful activity potential and were prioritized as computational evidence for molecular docking analysis (Widyananda *et al.*, 2021).

Molecular Docking Analysis

Ligands that have been tested for similarity to drug compounds and analyzed for toxicity are then analyzed using blind docking simulations. Ligand and protein docking is performed using AutoDock Vina in PyRx software. The initial process includes docking ligands from the *L. leucocephala* compound and a control ligand (isoniazid) to the inhA receptor (Chen *et al.*, 2020). The ligand binding process to the target protein provides data and information about the interaction patterns involved. The best docking analysis result is determined by the lowest binding affinity (Aljahdali *et al.*, 2021). Although isoniazid resistance is known to arise from mutations in InhA, docking against mutant InhA structures was beyond the scope of this initial screening study and is recommended for future investigations.

Interaction Analysis and Visualization

Ligand-receptor interactions were visualized and analyzed using BIOVIA Discovery Studio Visualizer software. Visualization results were analyzed to determine residues, interaction types, and interaction categories, as well as the distance between the target protein and the ligand. Hydrogen and hydrophobic bonds were identified to evaluate binding stability and potential inhibitory effects (Haque *et al.*, 2022). The docking results visualized were those with the lowest binding affinity. This visualization aims to evaluate the docking results in detail (Halder & Elma, 2021).

Molecular Dynamics Simulation Analysis

Molecular dynamics simulation was conducted to evaluate the stability of the molecular docking results and ligand–protein interactions using the CABS-flex 2.0 web server (https://biocomp.chem.uw.edu.pl/CABSflex2/index) (Herdiasyah *et al.*, 2024). The simulation employed established parameters, including protein rigidity (1.0), protein restraints (ss2 3 3.8 8.0), global C-alpha restraint weight (1.0), number of cycles (50), trajectory cycle interval (50), temperature range (1.4), and RNG seed (227) (*Shivanika et al.*, 2020; Nandana *et al.*, 2023). Receptor stability was assessed through root mean square fluctuation (RMSF) and radius of gyration (Rg) analyses, which served as indicators of structural flexibility and compactness (Aurora *et al.*, 2022). RMSF values within 1–3 Å were considered reflective of stable protein conformations throughout the simulation (Wijaya *et al.*, 2021), thereby supporting the reliability of the molecular docking outcomes.

Data Analysis

Each docking interaction result was downloaded and then analyzed to evaluate binding affinity and chemical bond type. Position and interaction analysis was performed using BIOVIA Discovery Studio Visualizer. The best-performing ligand-protein complexes were visualized in 2D and 3D to demonstrate the specific interaction types formed.

Results

A total of 73 phytochemicals were identified from *L. leucocephala* seeds based on literature reports (Elbanoby *et al*., 2022; Chargui *et al*., 2023; Verma *et al*., 2018; Nadhm & Al-Waheeb, 2024) and database searches. These compounds include alcohols (e.g., 1,2,3-propanetriol, phytol), furan derivatives (furaneol), and various saturated and unsaturated fatty acids and their esters, such as palmitic, stearic, linoleic, linolenic, arachidic, myristic, and behenic acids. Several phenolic compounds and flavonoids were also reported, including catechin, chlorogenic acid, vanillic acid, ferulic acid, rutin, ellagic acid, rosmarinic acid, and myricetin. Additionally, alkaloids (e.g., cyclohexylpiperidine, dihydropinidine), sterols (β-sitosterol, lanosterol, dihydrobrassicasterol, stigmasta-5,22-dien-3-ol), and tocopherols (vitamin E) were detected. The diversity of these 73 phytochemicals highlights the potential of *L. leucocephala* seeds as a rich source of bioactive molecules suitable for *in silico* screening against Mtb.

InhA of Mtb was selected as the molecular target, as it plays a central role in the fatty acid biosynthesis pathway (FAS-II) and is directly involved in the production of mycolic acids, essential components of the mycobacterial cell wall. Its structure was retrieved from the RCSB Protein Data Bank and prepared for docking analysis.

Drug-likeness and toxicity evaluation of *L. leucocephala* seed phytochemicals showed that 11 compounds complied with molecular docking studies (Table 1).

Toxicity analysis using ProTox classified all compounds into Class VI, with LD_{50} values greater than 5000 mg/kg, which is categorized as "practically non-toxic." The highest LD_{50} values (20,000 mg/kg) were observed in linoleic acid methyl ester, ethyl linoleate, linoleic acid butyl ester, 9,12-Octadecadienoic acid methyl ester, and linoleic acid ethyl ester. Catechin, a flavonoid compound, also demonstrated a favorable safety profile with an LD_{50} value of 10,000 mg/kg. Overall, these results suggest that the secondary metabolites of *L. leucocephala* seeds are safe and possess promising pharmacological potential for further anti-tuberculosis investigations.

Antimycobacterial and antituberculosis probability analysis using PASS Online revealed that Diethyl phthalate, linoleic acid methyl ester, linoleic acid, ethyl linoleate, linoleic acid-butyl ester, 9,12-Octadecadienoic

Table 1. Drug-Likeness Identification and Results of Toxicity Analysis

Phytochemical	Drug-Likness Identification						Toxicity activity	
	MW (<500) g/mol	HA (<10)	HD (<5)	LogP(<5)	Lipinski	Voliation	Class	LD50 (mg/kg)
Diethyl phthalate	222.24	4	0	2.30	Yes	0	6	6172
Linoleic acid methyl ester	294.47	2	0	2.30	Yes	1	6	20000
Linoleic acid	280.45	2	1	2.30	Yes	0	6	10000
Ethyl linoleate	308.50	2	0	2.30	Yes	1	6	20000
Linoleic acid, butyl ester	336.55	2	0	2.30	Yes	1	6	20000
Carbonic acid, dimethyl ester	90.0	3	0	0.35	Yes	0	6	6000
Propanedioic acid, dimethyl ester	132.11	4	0	0.18	Yes	0	6	5331
9,12-Octadecadienoic acid (Z,Z)-, methyl ester	294.47	2	0	0.18	Yes	0	6	20000
Linoleic acid ethyl ester	308.50	2	0	0.18	Yes	0	6	20000
Catechin	290.27	6	5	0.83	Yes	0	6	10000
Linolenic acid	278.43	2	1	0.83	Yes	0	6	10000

Table 2. Antimycobacterial and Antituberculosis Probability PrediAntituberculosisction

Bioactive Compound	Antimycobacterial dan Antituberculosis	
	Antimycobacterial	Antituberculosis
Diethyl phthalate	0,329	0,368
Linoleic acid methyl ester	0,407	0,355
Linoleic acid	0,440	0,424
Ethyl linoleate	0,464	0,458
Linoleic acid, butyl ester	0,418	0,383
Carbonic acid, dimethyl ester	-	-
Propanedioic acid, dimethyl ester	0,330	0,231
9,12-Octadecadienoic acid (Z,Z)-, methyl ester	0,407	0,355
Linoleic acid ethyl ester	0,464	0,458
Catechin	0,252	0,236
Linolenic acid	0,473	0,443

acid (Z,Z)-methyl ester, linoleic acid-ethyl ester and linolenic acid exhibited Pa > 0.3 (Table 2). These scores indicate that the bioactive compounds possess a higher likelihood of exerting antituberculosis activity. Therefore, these compounds were prioritized for further bioinformatics investigation. However, the predictive results still require validation through *in vitro* and *in vivo* studies. Additionally, the compounds selected for docking against four Mtb target proteins complied with demonstrated strong antituberculosis probability.

Molecular docking was performed to evaluate the interactions between selected phytochemical compounds from *L. leucocephala* seeds and the inhA protein from Mtb, with isoniazid as the reference ligand (control). A total of eight bioactive compounds were docked based on selection in the previous stage. The docking scores, which represent binding affinity, are presented in Table 3.

Table 3. Docking Results of Selected Phytochemical from *L. leucocephala* Seeds toward inhA Protein

Phytochemical	PubChem CID / HMDB ID	Binding Affinity (kcal/mol)
Isoniazid (Control)	**HMDB0015086**	**-5,8**
Diethyl phthalate	**6781**	**-7,5**
Linoleic acid methyl ester	5284421	-6,6
Linoleic acid	5280450	-6,6
Ethyl linoleate	5282184	-6,2
Linoleic acid, butyl ester	6436910	-5,9
-9,12-Octadecadienoic acid (Z,Z)-, methyl ester	5284421	-6,9
Linoleic acid ethyl ester	5282184	-6,0
Linolenic acid	52800934	-6,4

The docking results demonstrated that most of the tested phytochemicals exhibited stronger binding affinities than isoniazid (−5.8 kcal/mol). Among them, diethyl phthalate (−7.5 kcal/mol), indicating a strong interaction with the active site of inhA protein. Other compounds, such as -9,12-octadecadienoic acid methyl ester (−6.9 kcal/mol), linoleic acid and its derivatives (−6.0 to −6.6 kcal/mol), also displayed favorable binding energies compared to the control ligand.

In contrast, carbonic acid dimethyl ester (−3.7 kcal/mol) exhibited the weakest binding affinities, suggesting limited inhibitory potential. Overall, the results indicate that diethyl phthalate derivatives are the most promising candidates for further investigation as potential inhibitors of the inhA protein in Mtb.

Molecular docking visualization was carried out to further explore the interaction between the top-binding phytochemicals from *L. leucocephala* seeds and the inhA protein of Mtb. The three-dimensional (3D) and two-dimensional (2D) interaction diagrams provide detailed insights into the binding mode, hydrogen bond formation, hydrophobic interactions, and van der Waals forces involved in ligand–protein complexes (Figure 3) illustrates the binding interactions of diethyl phthalate and isoniazid (control).

The interaction analysis between diethyl phthalate and the reference drug isoniazid with the inhA protein revealed distinct binding profiles (Table 4). Diethyl phthalate exhibited a simpler interaction profile but still maintained significant binding with the target protein. It established one conventional hydrogen bond with GLY96, together with hydrophobic contacts such as Pi–alkyl with VAL65 and ILE95, Pi–Pi stacking with PHE41, and Pi–sigma interactions with ILE122. Importantly, interaction analysis did not reveal any

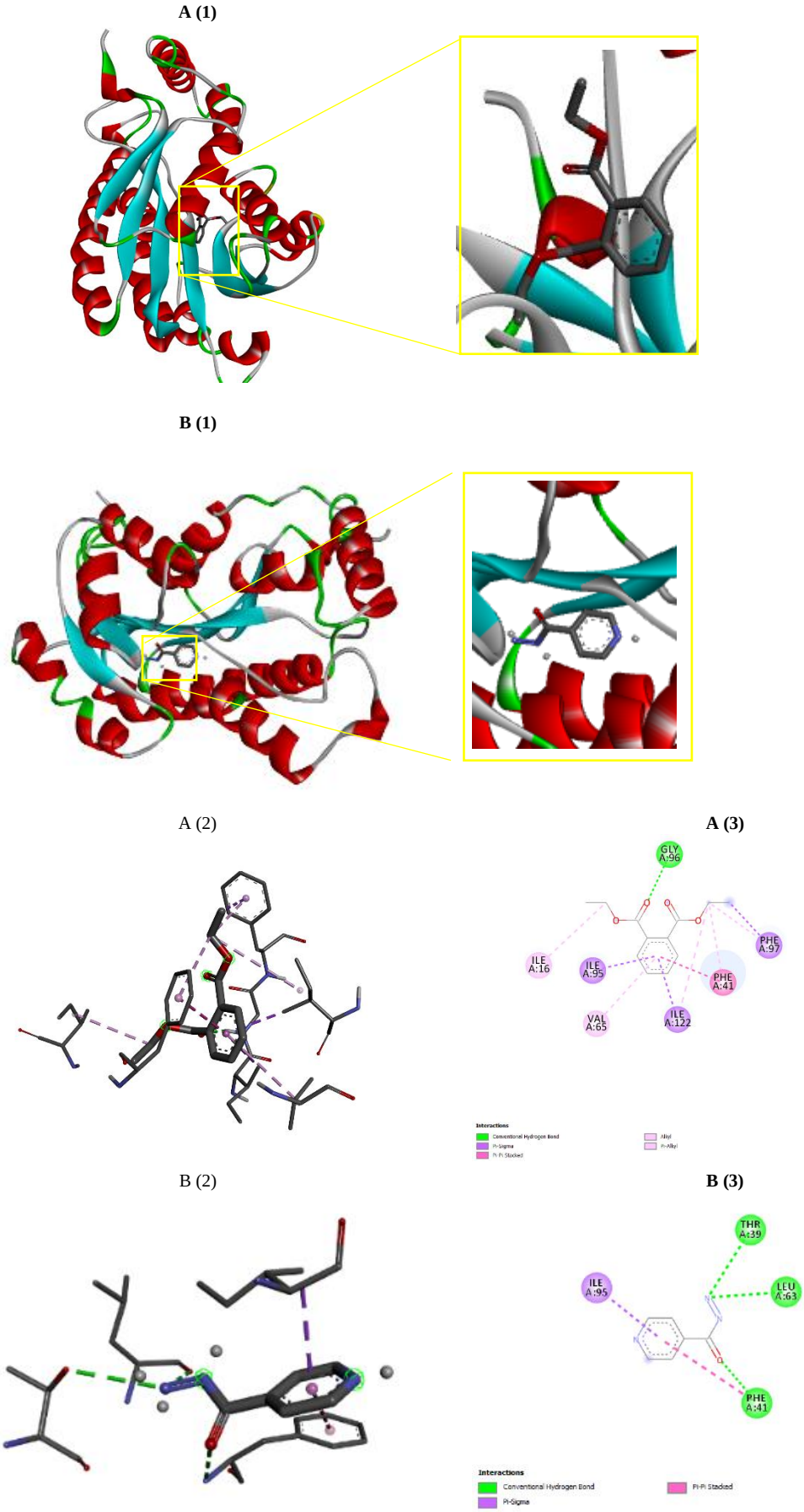


Fig. 3. Protein–ligand interaction results after molecular docking against inhA protein. (A) Diethyl phthalate: (1) ligand–protein binding interaction, (2) 3D structure of the complex, (3) 2D interaction diagram (B) Isoniazid: (1) ligand–protein binding interaction, (2) 3D structure of the complex, (3) 2D interaction diagram

Table 4. Interaction ligand and receptor

Ligand	Residues	Distance (A)	Interaction	
			Category	Type
Diethyl phthalate	ILE 16	3,89	Hydrophobic	Alkyl
	ILE 95	3,94		Pi-Sigma
	ILE 122	3,80		
	PHE 97	3,72		
	PHE 41	4,00		Pi-Pi Stacked
	VAL 65	4,91		Pi-Alkyl
	GLY 96	3,28	Hydrogen Bond	Conventional Hydrogen Bond
Isoniazid	ILE 95	3,65	Hydrophobic	Pi-Sigma
	PHE 41	3,29	Hydrogen Bond	Conventional Hydrogen Bond
	THR 39	3,27		
	LEU 63	2,88		

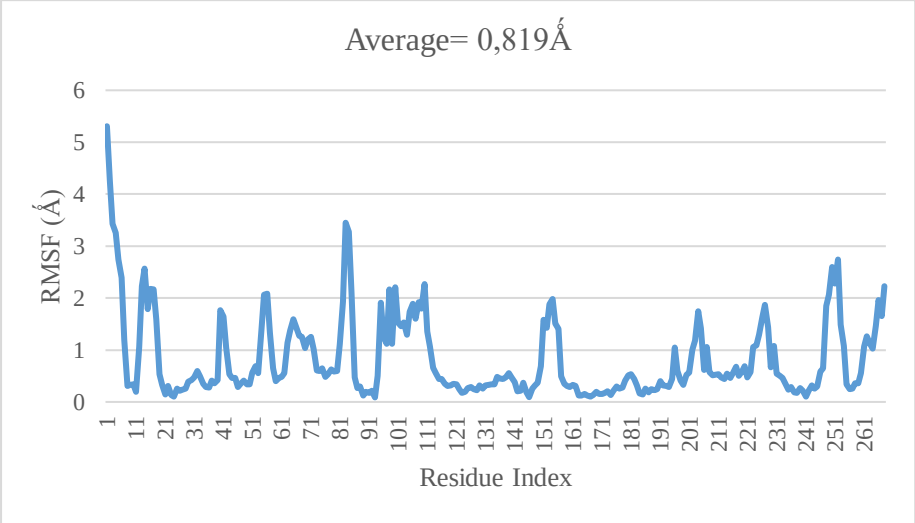


Fig. 4. Molecular dynamics analysis results of diethyl phthalate

unfavourable or disallowed interactions, such as steric clashes or repulsive donor–donor or acceptor–acceptor contacts, in the diethyl phthalate–inhA complex. The absence of such interactions suggests that the predicted binding pose is structurally compatible and energetically stable.

and Pi–sigma interactions with ILE122. Importantly, interaction analysis did not reveal any unfavourable or disallowed interactions, such as steric clashes or repulsive donor–donor or acceptor–acceptor contacts, in the diethyl phthalate–inhA complex. The absence of such interactions suggests that the predicted binding pose is structurally compatible and energetically stable.

In contrast, isoniazid formed three conventional hydrogen bonds with residues PHE41, THR39, and LEU63, alongside a Pi–sigma interaction with ILE95. While these interactions confirm its known inhibitory activity, the interaction network was less complex compared to diethyl phthalate , consistent with its lower docking score.

Overall, diethyl phthalate displayed the strongest and most versatile interaction profile among the tested compounds and the standard drug isoniazid. These findings further validate catechin as a promising lead compound for *inhA* inhibition in Mtb.

Molecular dynamics results showed that diethyl phthalate has an average RMSF value of 0.819 Å, indicating noticeable fluctuation across various residue positions (Figure 4). Several residues at the N-terminal region exhibited higher flexibility, reaching RMSF values above 4 Å, while most residue positions remained within the 0.5–2.0 Å range. These fluctuations suggest partial instability of the ligand–protein interaction throughout the simulated timeframe.

The present study highlights the potential of *L. leucocephala* seed phytochemicals as promising inhibitors of InhA, a key enzyme in the fatty acid synthase II (FAS-II) pathway of Mtb. InhA catalyzes the elongation of fatty acids required for mycolic acid biosynthesis, an essential component of the mycobacterial cell wall. Disruption of this pathway compromises cell wall integrity and bacterial survival, making InhA a validated therapeutic target (Vilchèze & Jacobs, 2019).

Based on the interaction diagram we provided, no unfavorable or disallowed interactions are shown. An analysis of the ligand-protein interaction map of Diethyl phthalate revealed no unfavorable or disallowed interactions. All identified interactions, including hydrogen bonds, pi-sigma, Pi-Pi stacking, and alkyl/Pi-alkyl interactions, are favorable and support the stability of the protein-ligand complex. The absence of unfavorable interactions indicates that the ligand has the potential to form a stable complex without adverse steric or electrostatic hindrance.

These results align well with other recent *in silico* studies in which flavonoid and polyphenolic scaffolds frequently emerged as top candidates in virtual screening pipelines targeting InhA. For instance, Singh & Pandey (2022) conducted a screening of plant-derived

metabolites and found that certain flavonoids exhibited binding energies comparable to or stronger than isoniazid, supported by favorable interactions with active site residues. Similarly, Bhaskar *et al.* (2023) used 3D-QSAR, virtual screening, and molecular dynamics simulations to identify novel InhA inhibitors derived from natural compound libraries, highlighting the role of multi-point hydrogen bonding and hydrophobic networks in enhancing inhibitor potency.

Diethyl phthalate also demonstrated favorable binding energy (−7.5 kcal/mol) with stable interactions involving hydrogen bonding (GLY96) and hydrophobic contacts (PHE41, ILE95, and VAL65). The presence of both hydrogen bonds and hydrophobic forces indicates potential as a secondary inhibitor. Conversely, isoniazid exhibited fewer interactions, forming three hydrogen bonds (PHE41, THR39, LEU63) and one Pi–sigma contact (ILE95), which may explain its relatively weaker docking score despite its proven clinical efficacy. This observation aligns with recent computational studies reporting that natural compounds often exhibit broader interaction networks with InhA compared to isoniazid, potentially contributing to stronger *in silico* binding affinities.

Diethyl phthalate (DEP) is a widely used plasticizer that has recently attracted scientific interest for its possible biological activities, although evidence remains controversial. Some studies report that DEP exhibits antimicrobial potential through quorum-sensing inhibition in *Chromobacterium violaceum* and *Pseudomonas aeruginosa*, as well as cytotoxic effects against breast cancer cells (MDA-MB-231) with an IC_{50} of approximately 65 µg/mL (Premjanu & Jaynthy, 2014; Srinivasan *et al*., 2025). In neuronal cell models, DEP has been shown to enhance apoptosis under nutrient stress by upregulating Bax expression, promoting cytochrome c release, and activating caspase-3 (Sun *et al*., 2012). Despite these preliminary findings suggesting potential antimicrobial and anticancer properties, most experimental and toxicological studies emphasize the adverse health effects of DEP. Chronic or high-dose exposure is associated with oxidative stress, inflammation, endocrine disruption, hepatotoxicity, adipocyte dysfunction, and developmental toxicity in animal and cell models (Lee *et al*., 2014; Mondal *et al*., 2023; Seo *et al*., 2025). Therefore, while DEP may demonstrate limited bioactivity *in vitro*, the overall body of evidence positions it primarily as an environmental contaminant and toxicant rather than a safe therapeutic candidate.

The results also highlight the potential contribution of linoleic acid derivatives, which showed moderate binding affinities (−6.0 to −6.6 kcal/mol). These compounds mainly interacted through hydrophobic forces, consistent with the known antibacterial mechanisms of polyunsaturated fatty acids, which include enzyme inhibition and membrane destabilization (Desbois & Smith, 2010; Elbanoby *et al*., 2022). While individually less potent than catechin, their presence in crude extracts may provide synergistic antimicrobial effects.

The RMSF analysis provides insights into the structural mobility of the protein backbone during ligand binding. An average RMSF value below 1 Å generally indicates stable interactions, while higher values suggest increased flexibility and lower stability. In this study, the average RMSF of 0.819 Å indicates borderline stability; however, the presence of several highly fluctuating residues (>3 Å) implies that diethyl phthalate may not maintain a consistently strong binding pose within the active site.

Peaks observed at the N-terminal and certain loop regions suggest conformational adjustments that may weaken binding affinity. Such instability could reduce inhibitory efficiency under physiological conditions, particularly when compared to ligands with lower dynamic fluctuations reported in previous InhA–inhibitor simulations. Therefore, although diethyl phthalate performed well in docking analysis, its dynamic behavior suggests that additional optimization or modification of the chemical structure may be required to enhance interaction stability.

Although computational screening provides an important first step, these findings must be validated through integrated experimental pipelines. Critical next steps include molecular dynamics simulations to assess complex stability under dynamic environments, GC–MS/LC–MS verification to confirm endogenous DEP presence in the extract, in vitro InhA inhibition and bacterial susceptibility assays for activity confirmation, and comprehensive ADME/Tox studies with emphasis on chronic toxicity and endocrine impacts.

Overall, this work identifies DEP as a preliminary and cautionary chemical scaffold for InhA inhibition, suggesting a foundation for future structural optimization toward safer analogs. While not yet suitable as a direct therapeutic candidate, its promising docking performance highlights the drug discovery potential of *L. leucocephala* seeds as a source of new anti-tuberculosis molecular templates.

Conclusion

This *in silico* study successfully identified phytochemicals from *Leucaena leucocephala* seeds with the potential to inhibit the InhA enzyme of *Mycobacterium tuberculosis*. Through drug-likeness screening, toxicity profiling, biological activity prediction, and molecular docking analysis, diethyl phthalate (DEP) emerged as the strongest candidate, demonstrating the highest binding affinity and stable ligand–protein interactions within the InhA active site compared to the standard drug isoniazid. Molecular dynamic simulation demonstrated the lower stability. Future studies should verify the natural occurrence of DEP in the extract, evaluate its enzymatic and antimycobacterial activity, and assess pharmacokinetic and toxicological profiles.

References

Aljahdali MO., Molla MHR., and Ahammad F. 2021. Compounds identified from marine mangrove plant (*Avicennia alba*) as

potential antiviral drug candidates against WDSV, an in-silico approach. Marine Drugs 19(5): 253.

Aurora Y, Tarigan IPN., Suryanto NMM., Santosa P., Pricilla V., Parikesit AA. 2022. Identification of flavonoids of *Kalanchoe pinnata* as candidate drugs for COVID-19 gamma-varint treatment. Mal J Fund Appl Sci. 18(6):630-643.

Bageel A., Honda MD., Carrillo JT., and Borthakur D. 2020. Giant leucaena (*Leucaena leucocephala* subsp. glabrata): a versatile tree-legume for sustainable agroforestry. Agroforestry Systems 94(1): 251-268.

Banerjee P., Kemmler E., and Dunkel M. 2024. ProTox 3.0: a webserver for the prediction of toxicity of chemicals. Nucleic Acid Research 52(W1): W513-W520.

Bhaskar V., Kumar S., Sujathan Nair A., Gokul S., Rajappan Krishnendu P., Benny S., and Mathew B. 2025. *In silico* development of potential InhA inhibitors through 3D-QSAR analysis, virtual screening and molecular dynamics. Journal of Biomolecular Structure and Dynamics *43*(3): 1329-1351.

Chargui H., Ghazghazi H., Essghaier B., Ben Fradj MK., Feki M., Charfi I., Ben Salem R., Rigane G., and Bejaoui, Z. 2023. Investigation on the chemical composition of phenolic, fatty acid profiles (GC-FID) and biological activities from *Leucaena leucocephala* (Lam de Wit) seed oil and leaves extracts: Effect of geographical location and maturation stage. Chemistry Africa *6*(4): 819–826.

Chen G., Seukep AJ., and Guo M. 2020. Recent advances in molecular docking for the research and discovery of potential marine drugs. Mar Drugs 18(11): 545.

Desbois AP., and Smith VJ. 2010. Antibacterial free fatty acids: Activities, mechanisms of action and biotechnological potential. Applied Microbiology and Biotechnology *85*(6): 1629–1642.

Elbanoby NE., El-Settawy AAA., Mohamed AA., and Salem MZM. 2022. Phytochemicals derived from *Leucaena leucocephala* (Lam.) de Wit (Fabaceae) biomass and their antimicrobial and antioxidant activities: HPLC analysis of extracts. Biomass Conversion and Biorefinery 14: 14593–14609.

Halder SK., and Elma F. 2021. *In silico* identification of novel chemical compounds with antituberculosis activity for the inhibition of InhA and EthR proteins from *Mycobacterium tuberculosis*. Journal of Clinical Tuberculosis and Other Mycobacterial Diseases 24: 100246.

Haque A., Baig GA., Alshawli AS., Sait KHW., Hafeez BB., Tripathi MK., Alghamdi BS., Mohammed Ali HSH., and Rasool M. 2022. Interaction Analysis of MRP1 with Anticancer Drugs Used in Ovarian Cancer: *In Silico* Ap-proach. Life 12(3): 1–12.

Herdiansyah MA., Ansori ANM., Kharisma V.D., Alifiansyah MRT., Anggraini D., Priyono QAP., & Maksimiuk N. 2024. In silico study of cladosporol and its acyl derivatives as anti-breast cancer against alpha-estrogen receptor. Biosaintifika 16(1), 142-154.

Kautsar R., Rachmawati Y., Rokhim S., Sucipto TH., Damayanti M., and Ramadhani AH. 2024. *In silico* analysis of inhibitor potential of punicalagin compound in pomegranate (punica granatum) against NS5 DENV-3 protein. Indonesian Journal of Tropical and Infectious Disease 12(1): 24.

Lee, HJ., Choi, KC., and Jeung, EB. 2014. Diethyl phthalate has estrogenic activity in CHO and MCF-7 cells and affects uterine epithelial cell height in immature rats. Reproductive Toxicology 47: 51–59.

Mondal, S., Pal, S., & Chandra, AK. (2023). Diethyl phthalate, a plasticizer, induces adipocyte inflammation and apoptosis in mice after long-term dietary administration. Journal of Biochemical and Molecular Toxicology 37(8): e23561.

Nadhm SS., and Al-Waheeb AN. 2024. Evaluation of antibacterial and antioxidative properties of *Leucaena leucocephala* fruit extract and analysis of its composition using gas chromatography–mass spectrometry. Plants 14(1): 010.

Nandana PI., Rasyid H., Yustisia I., & Hakim L. 2023. Molecular docking studies of Brucein D as a potential inhibitor of the Bcl-2 anti-apoptotic protein. Bali Medical Journal 12(2), 2148-2152.

Pajk S., Živec M., Šink R., Sosič I., Neu M., Chung C., Martínez HM., Pérez HE., Álvarez GD., Álvarez RE., Mendoza LA., Castro PJ., Barros D., Ballell PL., Young RJ., Convery MA., Encinas L., and Gobec S. 2016. New Direct Inhibitors of InhA with Antimycobacterial Activity Based on a Tetrahydropyran Scaffold. European Journal of Medicinal Chemistry 112: 252–257.

Premjanu, N., and Jaynthy, C. 2014. Antimicrobial activity of diethyl phthalate – an in silico approach. Asian Journal of Pharmaceutical and Clinical Research, 7(1): 144–147.

Raies AB., and Bajic VB. 2016. *In silico* toxicology: Computational methods for the prediction of chemical toxicity. Wiley Interdiscip. Rev. Comput. Mol. Sci. 6: 147–172.

Seo, S., Park, J., and Kim, S. 2025. Diethyl phthalate induces inflammation in RAW264.7 macrophages via JNK and STAT signaling pathways. BMC Molecular and Cell Biology 26: 12.

Shivanika C., Kumar D., Ragunathan V., Tiwari P., & Sumitha A. 2020. Molecular docking, validation, dynamics simulations, and pharmacokinetic prediction of natural compounds against the SARS-CoV-2 main-protease. Journal of biomolecular structure & dynamics, 1.

Singh K., and Pandey A. 2022. Identification of Novel Inhibitor of Enoyl-ACP Reductase (InhA) from Plant-Derived Metabolites: An In-Silico Study. Antibiotics 11(8): 1038.

Šink R., Sosič I., Živec M., Fernandez MR., Turk S., Pajk S., Alvarez GD., Lopez REM., Gonzales CC., Rullas TJ., Angulo BI., Barros D., Ballell PL., Young RJ., Encinas L., and Gobec S. 2015. Design, Synthesis, and Evaluation of New Thiadiazole-Based Direct Inhibitors of Enoyl Acyl Carrier Protein Reductase (InhA) for the Treatment of Tuberculosis. Journal of Medicinal Chemistry 58(2): 613–624.

Srinivasan, V., Kumar, R., and Sharma, A. 2025. In silico and in vitro evaluation of diethyl phthalate as a quorum sensing inhibitor and its antitumor activity against MDA-MB-231 cells. Journal of Biomolecular Structure and Dynamics 43(2): 1–12.

Sun, Y., Takahashi, K., Hosokawa, T., Saito, T., and Kurasaki, M. 2012. Diethyl phthalate enhances apoptosis induced by serum deprivation in PC12 cells. Basic & Clinical Pharmacology & Toxicology 111(4): 242–248.

Verma VK., Prakash O., Malik S., and Rani KV. 2018. Phytochemical screening and bioactive potential of pod seed extracts of *Leucaena leucocephala* Linn. Pharmacognosy Research 9 (1): S34–S40.

Vilchèze C., and Jacobs WRJr. 2019. The Isoniazid Paradigm of Killing, Resistance, and Persistence in Mycobacterium tuberculosis. Journal of Molecular Biology 431(18): 3450-3461.

Widyananda MH, Pratama SK, Samoedra RS, Sari FN, Kharisma VD, Ansori ANM.2021. Molecular docking study of sea urchin (*Arbacia lixula*) peptides as multi-target inhibitors for non-small cell lung cancer-associated proteins. J Pharm Pharmacogn Res. 9(4):484–96.

Wijaya RM., Hafidzhah MA., Kharisma VD., Ansori ANM. 2021. Parikesit AA. COVID-19 in silico drug with *Zingiber officinale* natural product compound library targeting the Mpro protein. Makara J Sci. 25(3):162-171.

World Health Organization. 2020. WHO operational handbook on tuberculosis. Module 1: prevention - Tuberculosis preventive treatment. Geneva: World Health Organization.

World Health Organization. 2022. Global tuberculosis report. Geneva: World Health Organization.

World Health Organization. 2023. Global tuberculosis report 2023. Geneva: WHO.

Xia Y., Zhou Y., Carter DS., McNeil MB., Choi W., Halladay J., Berry PW., Mao W., Hernandez V., O'Malley T., Korkegian A., Sunde B., Flint L., Woolhiser LK., Scherman MS., Gruppo V., Hastings C., Robertson GT., Ioerger TR., Alley MRK. 2018. Discovery of a cofactor-independent inhibitor of *Mycobacterium tuberculosis* InhA. Life Science Alliance *1*(3): e201800025.

Yuiana M., Suyanto E., Turhadi T., and Fatchiyah F. 2025. *In Silico* exploration of β-Glucogallin from *Malacca Fruit* (*Phyllanthus emblica*) as a dual inhibitor of ACE and AT1R in Chronic Kidney Disease. Berkala Penelitian Hayati *31*(2): 119-128.